Reaction Dynamics

DOI: 10.1002/ange.201310612

# Gas-Phase Synthesis of the Benzyl Radical ($C_6H_5CH_2$)**

*Beni B. Dangi, Dorian S. N. Parker, Tao Yang, Ralf I. Kaiser,* and Alexander M. Mebel**

***Abstract:*** *Dicarbon ($C_2$), the simplest bare carbon molecule, is ubiquitous in the interstellar medium and in combustion flames. A gas-phase synthesis is presented of the benzyl radical ($C_6H_5CH_2$) by the crossed molecular beam reaction of dicarbon, $C_2(X^1\Sigma_g^+, a^3\Pi_u)$, with 2-methyl-1,3-butadiene (isoprene; $C_5H_8$; $X^1A'$) accessing the triplet and singlet $C_7H_8$ potential energy surfaces (PESs) under single collision conditions. The experimental data combined with ab initio and statistical calculations reveal the underlying reaction mechanism and chemical dynamics. On the singlet and triplet surfaces, the reactions involve indirect scattering dynamics and are initiated by the barrierless addition of dicarbon to the carbon–carbon double bond of the 2-methyl-1,3-butadiene molecule. These initial addition complexes rearrange via multiple isomerization steps, leading eventually to the formation of $C_7H_7$ radical species through atomic hydrogen elimination. The benzyl radical ($C_6H_5CH_2$), the thermodynamically most stable $C_7H_7$ isomer, is determined as the major product.*

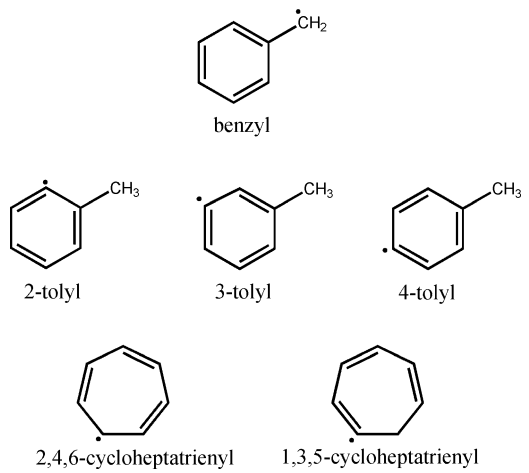


***Scheme 1.*** Structures of the most common $C_7H_7$ radicals.

Astrochemical and combustion models on the formation of polycyclic aromatic hydrocarbon (PAH) propose molecular weight growth processes through sequential reactions of aromatic (AR) and resonance-stabilized free radicals (RSFR), eventually leading to carbonaceous nanoparticles.[1,2] Along with acetylene, these pathways are considered as the basis for the hydrogen abstraction–acetylene addition (HACA),[3] phenyl addition–cyclization (PAC),[4] ethynyl addition (EA),[5] and vinylacetylene addition (VA)[6] mechanisms. Owing to their stability even at elevated temperatures of several thousand Kelvin, RSFRs and ARs can reach high concentrations in flames and in extraterrestrial environments, such as in circumstellar envelopes of carbon stars. These high concentrations make them important reaction intermediates to be involved in mass growth processes and hence in the formations of PAHs. During the last decade, particular focus has been directed to the role of the $C_7H_7$ radicals, including benzyl ($C_6H_5CH_2$), *o*-, *m*-, and *p*-tolyl (2-, 3-, and 4-tolyl; $C_6H_4CH_3$), and cycloheptatrienyl ($C_7H_7$) radicals (Scheme 1).[7–9] The benzyl radical ($C_6H_5CH_2$) has been proposed to yield indene ($C_9H_8$) upon reaction with acetylene ($C_2H_2$).[10,11] Indene may further produce indenyl radical(s). These indenyl radical(s) may then react with vinylacetylene ($C_4H_4$) to lead to fluorene, 1*H*-benz[f] indene, 1*H*-benz[e]indene, and/or 1*H*-phenalene. Owing to the potential key role of the benzyl ($C_6H_5CH_2$) radical, which is both aromatic and resonantly stabilized, in the formation of PAHs carrying five-membered rings, reaction mechanisms to distinct $C_7H_7$ isomers involving the phenyl radical ($C_6H_5$), fulvenallene ($C_7H_6$), 1-ethynyl-cyclopentadiene ($C_7H_6$), and the propargyl radical ($C_3H_3$) have been explored computationally.[7,8,12,13] However, the formation of $C_7H_7$ isomers (among them the thermodynamically most stable benzyl ($C_6H_5CH_2$) radical) via the bimolecular reaction of ubiquitous dicarbon molecules ($C_2$) with $C_5H_8$ isomers such as 2-methyl-1,3-butadiene (isoprene, $C_5H_8$; $X^1A'$) has never been reported. The dicarbon molecule is abundant in hydrocarbon flames and in the interstellar medium while the 2-methyl-1,3-butadiene can be formally derived from 1,3-butadiene ($C_4H_6$) by replacing the hydrogen atom at the C2 carbon atom by a methyl group. The 1,3-butadiene, together with its $C_4H_6$ isomers 1,2-butadiene, 1-butyne, and 2-butyne, is omnipresent in combustion flames, such as of ethylene and cyclohexane. Furthermore, $C_5H_8$ isomers have been probed in hydrocarbon flames, where the benzyl ($C_6H_5CH_2$) radical is determined as the major $C_7H_7$ species. Because of its resonant and aromatic stabilization, benzyl reaches significant concentrations in combustion flames and thus an understanding of its chemistry, in particular its formation and decomposition processes as well as bimolecular reactions, is essential for the development of accurate and predictive combustion engine models. Herein, we report the results of crossed molecular beams reaction of dicarbon with 2-methyl-1,3-butadiene accessing various

[*] Dr. B. B. Dangi, Dr. D. S. N. Parker, Dr. T. Yang, Prof. R. I. Kaiser
Department of Chemistry, University of Hawai'i at Manoa
Honolulu, HI 96822 (USA)
E-mail: ralfk@hawaii.edu
Homepage: http://www.chem.hawaii.edu/Bil301/welcome.html
Prof. A. M. Mebel
Department of Chemistry and Biochemistry
Florida International University, Miami, FL 33199 (USA)

[**] This work was supported by the US Department of Energy, Basic Energy Sciences, via grants DE-FG02-03ER15411 (Hawaii) and DE-FG02-04ER15570 (Florida).

Supporting information for this article is available on the WWW under http://dx.doi.org/10.1002/anie.201310612.

  

chemically activated reactive intermediates on the singlet and triplet $C_7H_8$ surfaces, which then decompose to products including distinct $C_7H_7$ isomers. These systems are also interesting from the viewpoint of a physical–organic chemist as they are benchmarks to unravel the chemical reactivity, bond breaking processes, and the synthesis of truly combustion and astrochemically relevant cyclic and aromatic hydrocarbon radicals from acyclic precursors via bimolecular gas-phase reactions in single collision events.

Reactive scattering signal from the reactions of dicarbon ($C_2$; 24 amu) with 2-methyl-1,3-butadiene ($C_5H_8$; 68 amu) was observed at $m/z = 91$ ($C_7H_7^+$), $m/z = 90$ ($C_7H_6^+$) and $m/z = 89$ ($C_7H_5^+$) with data at $m/z = 89$ depicting the best signal-to-noise ratio. The time-of-flight (TOF) spectra at these mass-to-charge rations were superimposable after scaling, suggesting that signal at $m/z = 90$ and 89 originated from dissociative ionization of the $C_7H_7$ product in the electron impact ionizer of the detector; if TOF data at two mass-to-charge ratios ($m/z$) are overlapping, data at lower $m/z$ are fragments from higher $m/z$. Therefore, our data suggest that only the dicarbon versus atomic hydrogen exchange channel is open, and that the molecular hydrogen loss pathways are closed. It should be emphasized that apart from dicarbon, the primary beam also contains atomic carbon and tricarbon molecules; however, tricarbon is unreactive with isoprene and hence does not interfere with the scattering signal obtained at lower mass-to-charge ratios. This is evident from the lack of any reactive scattering signal at $m/z = 103$ ($C_8H_7^+$), 102 ($C_8H_6^+$), and 101 ($C_8H_5^+$). Furthermore, signals at $m/z = 91$, 90, and 89 cannot be fit with a reactant mass combination of 36 amu (tricarbon) plus 68 amu (isoprene); therefore, this signal does not originate from dissociative ionization of any reactively scattered products in the tricarbon–$C_5H_8$ system. Likewise, ground state carbon atoms would react with the $C_5H_8$ isomer to products with molecular masses of 79 amu and less; therefore, reactions of carbon does not contribute to scattering signal at $m/z = 91$ to 89. Figure 1 presents selected TOF spectra recorded at various angles in the laboratory frame for the most intense fragment ion $m/z = 89$ ($C_7H_5^+$). These TOF spectra can be integrated to derive the laboratory angular distribution of the $C_7H_7$ product(s); this distribution peaks close to the center-of-mass (CM) angle of $44.1 \pm 1.3°$ and depicts a nearly forward–backward symmetric distribution extending at least 40° with the scattering plane defined by both beams. These patterns indicate indirect scattering dynamics through the formation of $C_7H_8$ reaction intermediates on the singlet and triplet surfaces. In summary, the interpretation of the TOF data alone suggests the existence of dicarbon versus hydrogen atom exchange channel(s) and the formation of $C_7H_7$ isomer(s).

First, we would like to interpret the experimental data and present the information, which can be obtained from the crossed molecular beam experiments. For this, the laboratory data are converted into the center-of-mass (CM) reference frame to obtain the translational energy ($P(E_T)$) and angular ($T(\theta)$) distributions as shown in Figure 2. The $P(E_T)$ peaks slightly away from zero translational energy at around 20–30 kJ mol$^{-1}$, suggesting that at least one channel holds a tight exit transition state upon decomposition of the $C_7H_8$ intermediate(s);[14] this process is connected with a significant electron rearrangement upon the formation of the $C_7H_7$ product. Furthermore, the maximum of the translational energy of the $P(E_T)$ resembles the sum of the collision energy plus the reaction energy for those product molecules without internal excitation. Therefore, the maximum translational energy releases can be utilized to extract the reaction energy, and thus upon comparison with computed reaction energies also the structural isomer formed. Considering the maximum translational energy of $525 \pm 30$ kJ mol$^{-1}$, the reaction is determined to be exoergic by $482 \pm 32$ kJ mol$^{-1}$ after subtracting the nominal collision energies (Supporting information). Recall that the dicarbon beam also holds molecules in its first electronically excited state $a^3\Pi_u$, which lies higher by 8 kJ mol$^{-1}$ compared to its $X^1\Sigma_g^+$ ground state.[15] Therefore, a subtraction of this energy indicates that the reaction of dicarbon with 2-methyl-1,3-butadiene is exoergic by $474 \pm 32$ kJ mol$^{-1}$. Finally, the translational energy distribution helps to calculate the averaged fraction of available energy released into the translational degrees of freedom to be $26 \pm 5$%; this order of magnitude proposes indirect reaction dynamics.[16] The $T(\theta)$ distribution is forward–backward

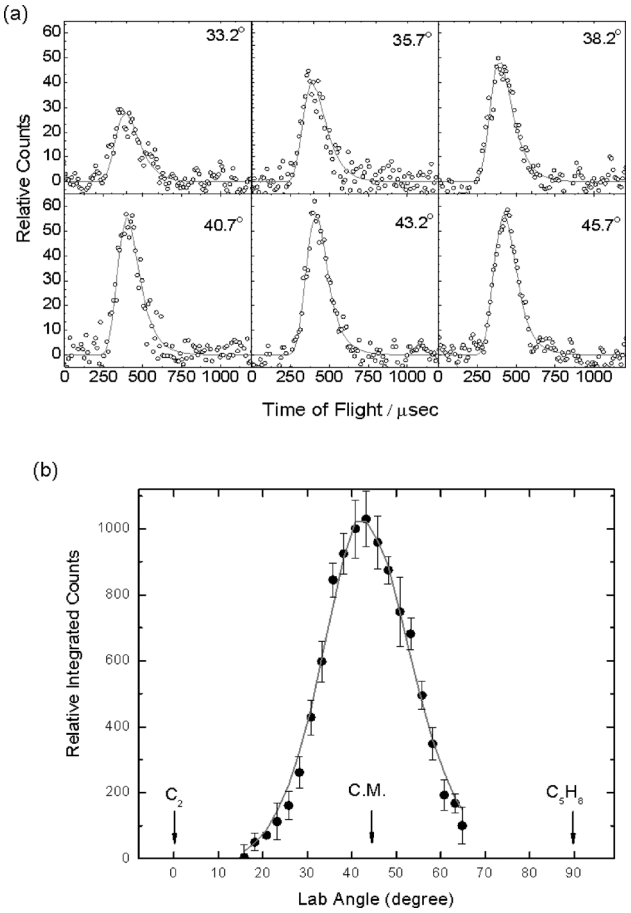


***Figure 1.*** Time-of-flight data (a) and laboratory angular distribution (b) at $m/z = 89$ ($C_7H_5^+$) for the reaction of dicarbon ($C_2$) with isoprene ($C_5H_8$) forming $C_7H_7$ product(s) at collision energy of $42.7 \pm 1.5$ kJ mol$^{-1}$. The circles represent the experimental data, error bars present the standard deviation, and the solid lines represent the fit.

  

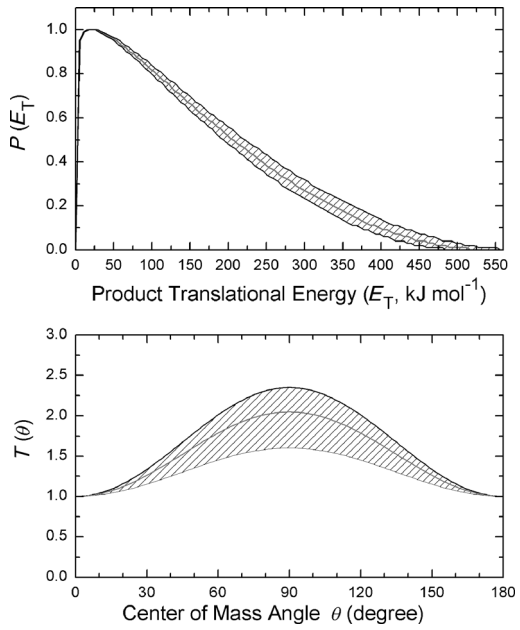


***Figure 2.*** Center-of-mass translational energy flux distribution (upper) and angular distribution (lower) for the hydrogen atom loss channel in the reaction of dicarbon with isoprene leading to $C_7H_7$ product(s). Hatched areas indicate the acceptable upper and lower error limits of the fits and solid gray middle lines define the best-fit functions.

symmetric with respect to 90° and is distributed over the complete angular range of 0° to 180°. This finding suggests that this reaction follows indirect scattering dynamics via the formation of $C_7H_8$ reaction intermediate(s). Also, the distribution maximum of the center-of-mass angular distribution at 90° indicates "sideways scattering", that is, the departing atomic hydrogen atom is emitted preferentially perpendicularly with respect to the rotational plane of the decomposing complex.[17] This finding is also reflected in the flux contour map (see the table of contents graphic).

Second, we also explored the reaction of singlet and triplet dicarbon with isoprene computationally; the singlet and triplet $C_7H_8$ potential energy surfaces (PESs) are presented in Figure 3 and Figure 4. Considering the singlet surface, dicarbon can add without an entrance barrier to either the C3−C4 or the C1−C2 carbon–carbon double bonds of isoprene, yielding intermediates **si1** and **si2**, respectively. These collision complexes ring open to **si3** and **si4**, respectively. Both acyclic intermediates may undergo hydrogen shifts, yielding eventually intermediate **si5**, which then undergoes a *trans–cis* conversion to **si6** through a low barrier of only 21 kJ mol$^{-1}$. A hydrogen shift in the latter yields **si7**, which subsequently isomerizes via *cis–trans* conversion to **si8**. This intermediate can undergo ring closure to **si9** or **si10**; the ring closure to the former is initiated with a 1,3-H atom shift from the methyl group. Considering the inherent barriers of 340 and 145 kJ mol$^{-1}$, the formation of **si10** should be preferential. This species depicts a hydrogen shift at the ring from the *para* to the *meta* position to **si11**, with the latter isomerizing via yet another hydrogen migration to **si12** (toluene). Toluene is the global minimum on the $C_7H_8$ potential energy surface and can undergo unimolecular decomposition involving atomic hydrogen loss via four simple bond-rupture processes. These form the benzyl radical ($C_6H_5CH_2$) and/or *o*-, *m*-, and/or *p*-tolyl radicals. The benzyl radical is thermodynamically more stable by about 94 kJ mol$^{-1}$ compared to the tolyl radicals due to resonance stabilization of the radical center. Note that **si1** and **si2** can also react to products other than $C_7H_7$ (Supporting Information, Figure S1).

Figure 4 shows the reaction paths for addition of triplet dicarbon to the isoprene. The triplet dicarbon can add without entrance barrier to the C4 and C1 carbon atoms of isoprene, yielding intermediates **ti1** and **ti2**, respectively, which are bound by 180 and 190 kJ mol$^{-1}$ with respect to the separated reactants. These intermediates isomerize via hydrogen shifts and ring closures involving **ti3**, **ti6**, **ti11**, **ti12**, and **ti13** to eventually form the cyclic structures **ti4**, **ti7**, **ti8**, and **ti10**. Considering the inherent barriers to isomerization, all isomerization pathways involving **ti3** and **ti12** yield **ti4**, with **ti7** leading to **ti10** and **ti8**. What is the fate of these cyclic intermediates? Intermediate **ti4** isomerizes via hydrogen shift to **ti5**, which then decomposes to the benzyl radical through a tight exit transition state located 16 kJ mol$^{-1}$ above the separated products. **ti8** and **ti10** preferentially decompose by atomic hydrogen losses yielding *m*- and *p*-tolyl radicals, respectively, or undergo distinct hydrogen shifts (via **ti9**) and then dissociate to the benzyl radical ($C_6H_5CH_2$) and/or *o*-, *m*-, and/or *p*-tolyl radicals, or phenyl plus the methyl radical ($CH_3$). Note that with the exception of the decomposition of **ti9** to the benzyl radical, all exit transition states are tight. Intermediates **ti1** and **ti2** can also decompose to acyclic products (Supporting information Figure S1); however, these pathways are energetically not favorable.

Having interpreted the experimental data and the potential energy surfaces, the experimental findings (reaction energies, exit barriers, indirect nature of the reaction mechanism, and geometry of the exit transition state) can be merged with the computational data. A comparison of the experimentally determined exoergicity of the reaction of dicarbon with 2-methyl-1,3-butadiene of $474 \pm 32$ kJ mol$^{-1}$ with the computed reaction energies ($477 \pm 10$ kJ) suggests the formation of at least the thermodynamically most stable $C_7H_7$ isomer: the benzyl radical ($C_6H_5CH_2$). Considering that the experimentally determined off-zero peaking at 20 to 30 kJ mol$^{-1}$ of the center-of-mass translational energy distribution suggests a tight exit transition state, the computational data propose that at least one decomposition pathway involves **ti5**. In this case, **ti5** undergoes hydrogen loss via a barrier located 16 kJ mol$^{-1}$ above the separated products; the unimolecular decomposition of **ti9** is barrierless and thus not expected to result in an off-zero peaking of the center-of-mass translational energy distribution. How can **ti5** be formed? Considering the triplet surface, **ti5** is most likely reached from **ti1** via **ti3** and **ti4** or from **ti2** via **ti11**, **ti12**, and **ti4** involving hydrogen migrations and cyclization. Based on these considerations, we can conclude that on the triplet surface, triplet dicarbon adds to the C4 or C1 carbon atom of 2-methyl-1,3-butadiene, yielding intermediates **ti1** and **ti2**, respectively. Intermediate **ti1** undergoes hydrogen migration to form **ti3**, which then ring-closes to **ti4**. Alternatively, **ti2** features a hydrogen shift to **ti11** followed by rotation around

  

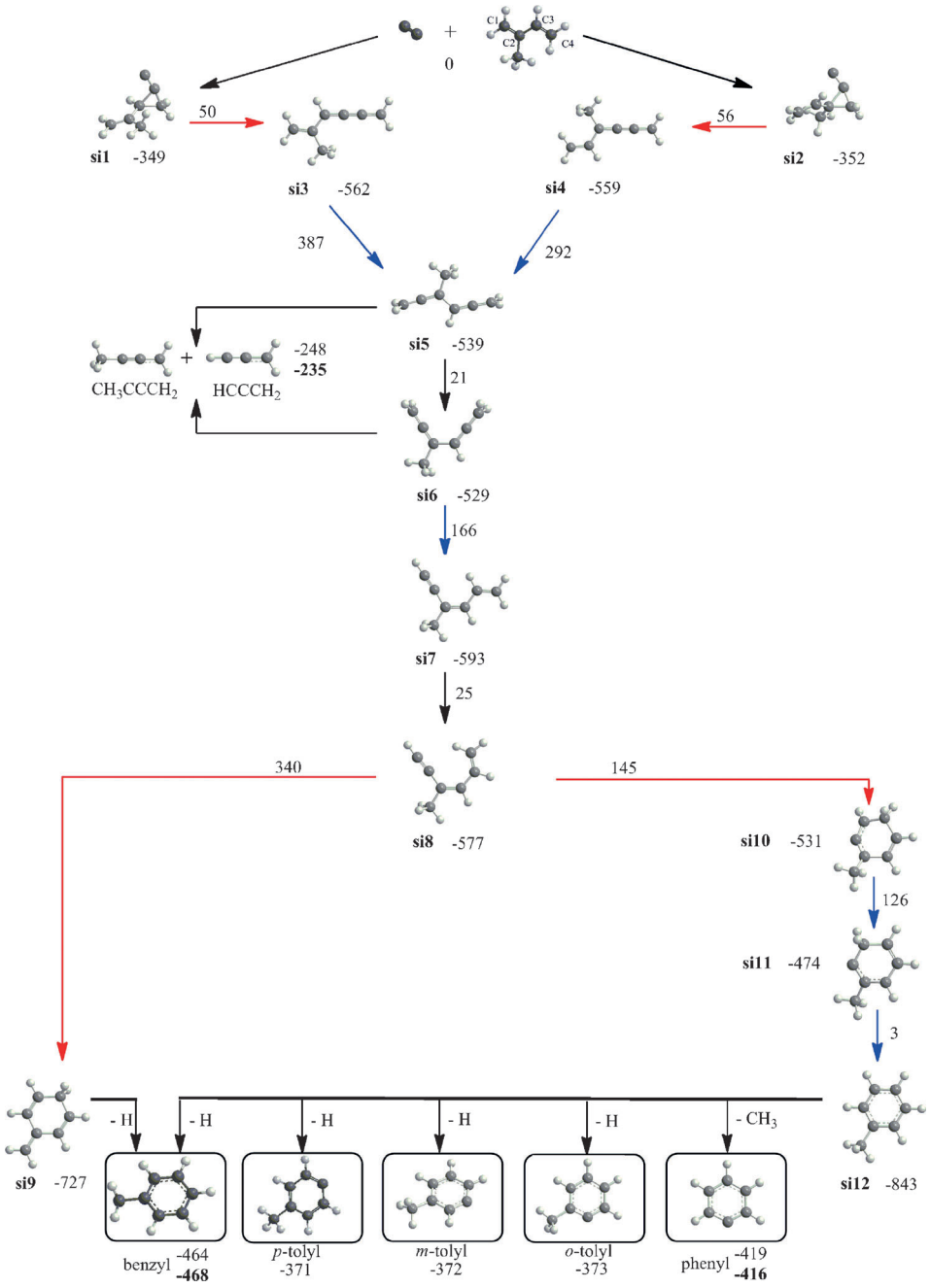


***Figure 3.*** Low-energy paths for the reaction of singlet dicarbon with isoprene leading to benzyl and tolyl products. Intermediates are labeled as **si** along with the energies relative to separated reactants and barrier heights, where applicable, in kJ mol$^{-1}$ as calculated at the CCSD(T)/CBS(dt)//B3LYP/6-311G**+ZPE (B3LYP/6-311G**) (plain numbers) and CCSD(T)/CBS(dtq)//B3LYP/6-311G**+ZPE(B3LYP/6-311G**) (bold numbers) levels of theory. Hydrogen shifts and isomerization via ring closure/opening are indicated with blue and red arrows, respectively. For clarification, the carbon atoms in isoprene are labeled as C1 to C4.

a C–C bond (to **ti12**) and a ring closure to **ti4**. This intermediate undergoes yet another hydrogen migration to **ti5**, which ultimately eliminates atomic hydrogen to form the benzyl radical. These indirect scattering dynamics were also predicted based on the center-of-mass angular distribution. Finally, recall that based on the center-of-mass angular distribution, the exit transition state was suggested to hold geometrical constraints depicting a hydrogen atom loss almost perpendicularly to the rotating plane of the decomposing complex. This finding was also confirmed computationally, predicting an angle of the hydrogen elimination of 81.3° (Figure 5). Note that based on the experimentally derived energetics alone, we cannot rule out the formation of thermodynamically less stable $C_7H_7$ radicals. Our statistical RRKM calculations predict that upon dicarbon addition to C1 under our experimental conditions, the benzyl radical dominates and is formed at fractions of about 61% with tolyl radicals contributing to about 37% with nearly equal contributions of *m*- and *p*-tolyl; furthermore, non-aromatic products are minor and contribute only 2%. Adding dicarbon to C4 produces about 25% benzyl and 75% *m*- and *p*-tolyl. The higher yield of benzyl computed for the C1 addition is determined by the fact that the barrier for the **ti2**→**ti11** isomerization eventually leading to **ti4** is 20 kJ mol$^{-1}$ lower than that for the competing **ti2**→**ti13** process, whereas the barriers for **ti1**→**ti3** on the path to **ti4** and **ti1**→**ti6** are nearly equal. If the C1 and C4 additions are equally split, we expect about 43% of benzyl.

The computations predict further that on the singlet surface, the addition to the C3–C4 and C1–C2 may eventually yield (via the collision complexes **si1** and **si2**) **si8** via a multi-step isomerization sequence involving successive hydrogen shifts. Considering the barrier to isomerization, intermediate **si8** is expected to rearrange to **si10**, which eventually yields singlet toluene (**si12**). The latter is expected to decompose via loose exit transition states to the benzyl as well as tolyl radicals, with a benzyl being formed preferentially. However, before intermediate **si8** can be even formed, the reaction can alternatively proceed by numerous fragmentation channels involving H, $CH_3$, and $C_3H_3$ elimination and the production of non-aromatic radicals (Supporting Informa-

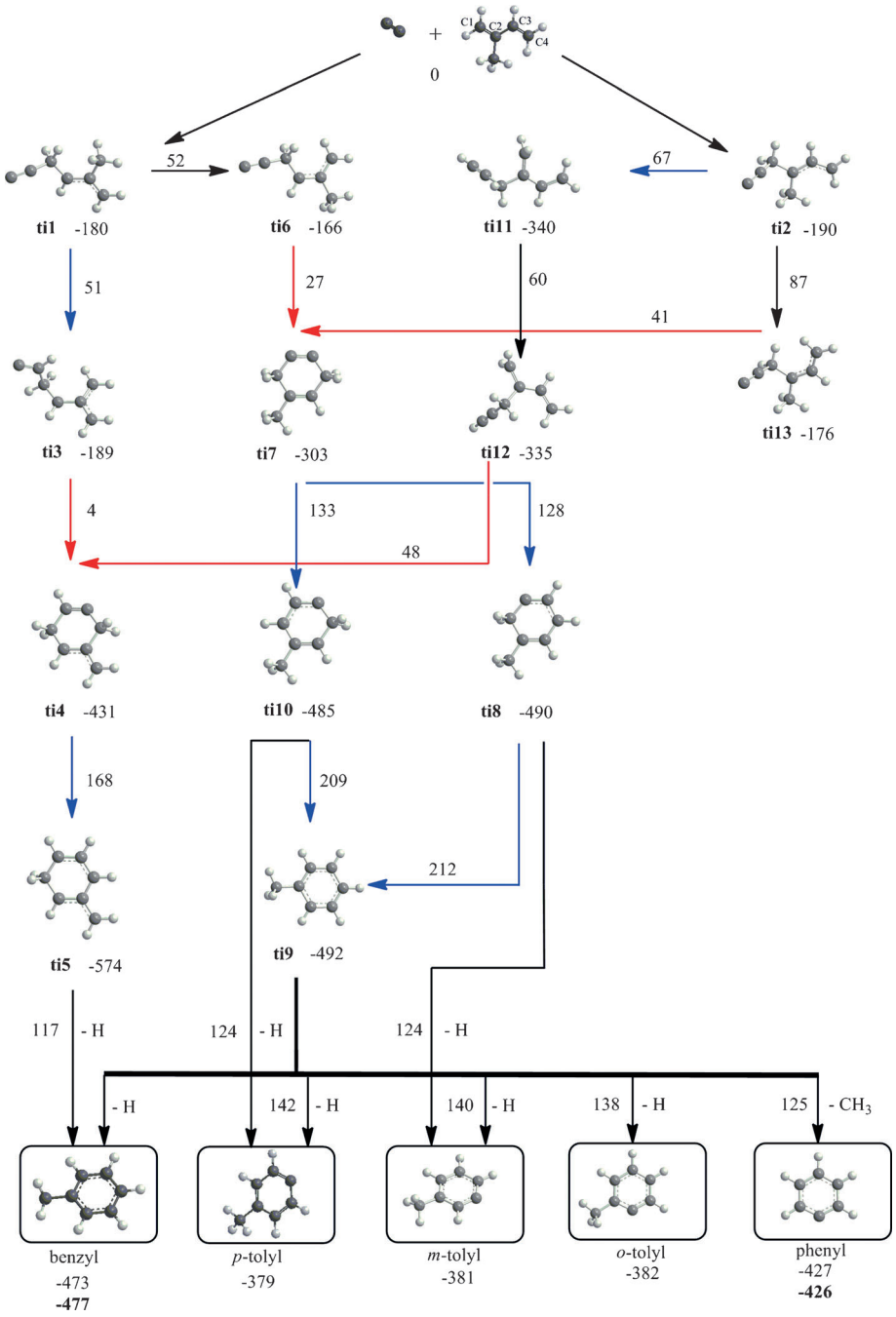


***Figure 4.*** Low-energy paths for the reaction of triplet dicarbon with isoprene leading to benzyl and tolyl products. Intermediates are labeled as **ti** along with the energies relative to separated reactants and barrier heights, where applicable, in kJ mol$^{-1}$ as calculated at the CCSD(T)/CBS(dt)//B3LYP/6-311G**+ZPE (B3LYP/6-311G**) (plain numbers) and CCSD(T)/CBS(dtq)//B3LYP/6-311G**+ZPE(B3LYP/6-311G**) (bold numbers) levels of theory. Hydrogen shifts and isomerization via ring closure/opening are indicated by blue and red arrows, respectively. For clarification, the carbon atoms in isoprene are labeled as C1 to C4.

tion, Figure S1). We conclude therefore that the addition of singlet dicarbon to the C3–C4 bond of 2-methyl-1,3-butadiene most likely forms non-aromatic $CH_2CCCHCCH_2$ plus methyl and **sp2**–**sp4** plus atomic hydrogen and the pathway from **si3** to the aromatic products is effectively closed. For **si4**, the barrier for the H shift to form **si5** is 292 kJ mol$^{-1}$, 46 and 54 kJ mol$^{-1}$ lower than the energies required for the $CH_3$ loss leading to $CH_2CHCCCCH_2$ and for the hydrogen loss producing **sp11**. Thus, the channel from **si4** to **si5** and then to **si8** and to benzyl can be in principle competitive. Nevertheless, we do not expect a high yield of benzyl from the singlet $C_2$ addition to the C1–C2 bond of 2-methyl-1,3-butadiene either. Our consideration is based on the comparison with the reaction of dicarbon with 1,3-butadiene earlier studied by us.[18] Computationally, the RRKM computed branching ratios were 44% for non-aromatic $C_6H_5$ radicals from the intermediate analogous to **si4**, 35% for propargyl plus propargyl (from the intermediate analogous to **si5**), and only 21% for the phenyl radical. The PES calculated for dicarbon plus 2-methyl-1,3-butadiene, from **si2** to **si4** and eventually to **si12**, is similar to that for dicarbon plus 1,3-butadiene, with methyl being merely a spectator group until **si12** is formed. Moreover, while the relative energy of the **si4**–**si5** transition state, which represents the bottleneck on the pathway to the aromatic products, is similar to that for its analogue in the dicarbon–1,3-butadiene reaction, the most favorable non-aromatic fragmentation products of **si4** reside 35–50 kJ mol$^{-1}$ lower in energy than their counterparts in the dicarbon–1,3-butadiene system and therefore the fragmentation processes of **si4** competing with its isomerization to **si5** should be relatively faster than for its analogue. Furthermore, **si4** can isomerize to **si15** via a barrier 7 kJ mol$^{-1}$ lower than that for **si4**→**si5** and **si15** can decompose to $CH_2CHCCH_2$ plus $C_3H_3$ or **sp11** plus atomic hydrogen further reducing the reaction flow to **si5** and eventually to **si12**. Therefore, we can suggest that the yield of benzyl radical from dicarbon addition to the C1–C2 bond of 2-methyl-1,3-butadiene should be less than 21%.

In summary, by merging the experimental and computational data, we provided compelling evidence that on the triplet surface the thermodynamically most stable aromatic and resonantly stabilized free radical benzyl is formed preferentially. This reaction provides a barrierless and

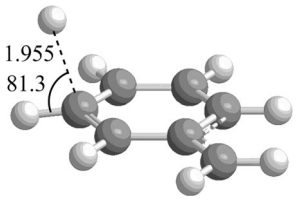


***Figure 5.*** Computed geometry of the exit transition state from intermediate **ti5** leading to the formation of benzyl radical.

hitherto overlooked reaction pathway via a single collision event from acyclic, non-aromatic reactants. As the reaction has no entrance barrier, is exoergic, and all transition states involved are located below the energy of the separated reactants, the reaction of triplet dicarbon with isoprene may form benzyl radical not only in high-temperature combustion flames, but also in low temperature astrochemical environments. On the other hand, on the singlet surface, the benzyl radical is expected to be of minor importance. Further, the replacement of a hydrogen atom by a methyl group in the 1,3-butadiene reactant leads to an active participation of the methyl group in the reaction dynamics to form the benzyl radical and not just purely a spectator. Therefore, reactions of simple C1 to C3 combustion relevant radicals are expected to follow a unique chemistry once reacting with methyl- and even alkyl-substituted reactants, which is anticipated to be remarkably distinct from their non-alkyl substituted counterparts.

Received: December 6, 2013
Revised: January 25, 2014
Published online: March 25, 2014

**Keywords:** benzyl radical · bimolecular reactions · combustion chemistry · gas-phase chemistry · reaction dynamics

[1] Z. A. Mansurov, *Combust. Explos. Shock Waves* **2005**, *41*, 727.
[2] I. Cherchneff, *Astron. Astrophys.* **2012**, *545*, A12.
[3] H. Bockhorn, F. Fetting, A. Heddrich, G. Wannemacher, *Ber. Bunsen-Ges.* **1987**, *91*, 819.
[4] M. Shukla, A. Susa, A. Miyoshi, M. Koshi, *J. Phys. Chem. A* **2008**, *112*, 2362.
[5] A. M. Mebel, V. V. Kislov, R. I. Kaiser, *J. Am. Chem. Soc.* **2008**, *130*, 13618.
[6] D. S. N. Parker, F. T. Zhang, Y. S. Kim, R. I. Kaiser, A. Landera, V. V. Kislov, A. M. Mebel, A. G. G. M. Tielens, *Proc. Natl. Acad. Sci. USA* **2012**, *109*, 53.
[7] G. da Silva, J. A. Cole, J. W. Bozzelli, *J. Phys. Chem. A* **2010**, *114*, 2275.
[8] M. Derudi, D. Polino, C. Cavallotti, *Phys. Chem. Chem. Phys.* **2011**, *13*, 21308.
[9] T. C. Zhang, L. D. Zhang, X. Hong, K. W. Zhang, F. Qi, C. K. Law, T. H. Ye, P. H. Zhao, Y. L. Chen, *Combust. Flame* **2009**, *156*, 2071.
[10] L. Vereecken, J. Peeters, *Phys. Chem. Chem. Phys.* **2003**, *5*, 2807.
[11] W. M. Davis, S. M. Heck, H. O. Pritchard, *J. Chem. Soc. Faraday Trans.* **1998**, *94*, 2725.
[12] S. J. Klippenstein, L. B. Harding, Y. Georgievskii, *Proc. Combust. Inst.* **2007**, *31*, 221.
[13] V. V. Kislov, A. M. Mebel, *J. Phys. Chem. A* **2007**, *111*, 3922.
[14] S. A. Safron, N. D. Weinstein, D. R. Herschbach, J. C. Tully, *Chem. Phys. Lett.* **1972**, *12*, 564.
[15] R. I. Kaiser, P. Maksyutenko, C. Ennis, F. T. Zhang, X. B. Gu, S. P. Krishtal, A. M. Mebel, O. Kostko, M. Ahmed, *Faraday Discuss.* **2010**, *147*, 429.
[16] R. D. Levine, *Molecular Reaction Dynamics*, Cambridge University Press, Cambridge, UK, **2005**.
[17] W. B. Miller, S. A. Safron, D. R. Herschbach, *Discuss. Faraday Soc.* **1967**, *44*, 108.
[18] F. T. Zhang, B. Jones, P. Maksyutenko, R. I. Kaiser, C. Chin, V. V. Kislov, A. M. Mebel, *J. Am. Chem. Soc.* **2010**, *132*, 2672.

  